Research Article | Vol. 25, No. 3 | 6 Feb 2017 | OPTICS EXPRESS 2950

Optics EXPRESS

Tungsten disulfide saturable absorbers for 67 fs mode-locked erbium-doped fiber lasers

WENJUN LIU,[1,2] LIHUI PANG,[2,3] HAINIAN HAN,[2,3] MENGLI LIU,[1] MING LEI,[1] SHAOBO FANG,[2,3] HAO TENG,[2,3,4] AND ZHIYI WEI[2,3,*]

[1]*State Key Laboratory of Information Photonics and Optical Communications, School of Science, P. O. Box 91, Beijing University of Posts and Telecommunications, Beijing 100876, China*
[2]*Beijing National Laboratory for Condensed Matter Physics, Institute of Physics, Chinese Academy of Sciences, Beijing 100190, China*
[3]*School of Physical Sciences, University of Chinese Academy of Sciences, Beijing 100190, China*
[4]*hteng@iphy.ac.cn*
[*]*zywei@iphy.ac.cn*

Abstract: In this paper, we demonstrate 67 fs pulse emitting with tungsten disulfide (WS_2) in mode-locked erbium-doped fiber (EDF) lasers. Using the pulsed laser deposition method, WS_2 is deposited on the surface of the tapered fiber to form the evanescent field. The fiber-taper WS_2 saturable absorber (SA) with the large modulation depth is fabricated to support the ultrashort pulse generation. The influences of the WS_2 SA are analyzed through contrastive experiments on fiber lasers with or without the WS_2 SA. The pulse duration is measured to be 67 fs, which is the shortest pulse duration obtained in the mode-locked fiber lasers with two dimensional (2D) material SAs. Compared to graphene, topological insulator, and other transition metal dichalcogenides (TMDs) SAs, results in this paper indicate that the fiber-taper WS_2 SA with large modulation depth is a more promising photonic device in mode-locked fiber lasers with the wide spectrum and ultrashort pulse duration.

OCIS codes: (160.4330) Nonlinear optical materials; (140.4050) Mode-locked lasers; (140.3510) Lasers, fiber.

References and links

1. M. Aliofkhazraei and N. Ali, *Two-Dimensional Nanostructures* (CRC, 2012).
2. Z. W. Pan, Z. R. Dai, and Z. L. Wang, "Nanobelts of semiconducting oxides," Science **291**(5510), 1947–1949 (2001).
3. S. Z. Butler, S. M. Hollen, L. Cao, Y. Cui, J. A. Gupta, H. R. Gutiérrez, T. F. Heinz, S. S. Hong, J. Huang, A. F. Ismach, E. Johnston-Halperin, M. Kuno, V. V. Plashnitsa, R. D. Robinson, R. S. Ruoff, S. Salahuddin, J. Shan, L. Shi, M. G. Spencer, M. Terrones, W. Windl, and J. E. Goldberger, "Progress, challenges, and opportunities in two-dimensional materials beyond graphene," ACS Nano **7**(4), 2898–2926 (2013).
4. M. E. Fermann and I. Hartl, "Ultrafast fibre lasers," Nat. Photonics **7**(11), 868–874 (2013).
5. L. E. Nelson, D. J. Jones, K. Tamura, H. A. Haus, and E. P. Ippen, "Ultrashort-pulse fiber ring lasers," Appl. Phys. B **65**(2), 277–294 (1997).
6. I. N. Duling, "All-fiber ring soliton laser mode locked with a nonlinear mirror," Opt. Lett. **16**(8), 539–541 (1991).
7. U. Keller, K. J. Weingarten, F. X. Kartner, D. Kopf, B. Braun, I. D. Jung, R. Fluck, C. Honninger, N. Matuschek, and J. Aus der Au, "Semiconductor saturable absorber mirrors (SESAM's) for femtosecond to nanosecond pulse generation in solid-state lasers," IEEE J. Sel. Top. Quantum Electron. **2**(3), 435–453 (1996).
8. A. A. Lagatsky, F. Fusari, S. Calvez, S. V. Kurilchik, V. E. Kisel, N. V. Kuleshov, M. D. Dawson, C. T. A. Brown, and W. Sibbett, "Femtosecond pulse operation of a Tm,Ho-codoped crystalline laser near 2 microm," Opt. Lett. **35**(2), 172–174 (2010).
9. J. Wang, Z. Cai, P. Xu, G. Du, F. Wang, S. Ruan, Z. Sun, and T. Hasan, "Pulse dynamics in carbon nanotube mode-locked fiber lasers near zero cavity dispersion," Opt. Express **23**(8), 9947–9958 (2015).
10. Q. L. Bao, H. Zhang, Y. Wang, Z. H. Ni, Y. L. Yan, Z. X. Shen, K. P. Loh, and D. Y. Tang, "Atomic-layer graphene as a saturable absorber for ultrafast pulsed lasers," Adv. Funct. Mater. **19**(19), 3077–3083 (2009).
11. H. Zhang, D. Y. Tang, L. M. Zhao, Q. L. Bao, and K. P. Loh, "Large energy mode locking of an erbium-doped fiber laser with atomic layer graphene," Opt. Express **17**(20), 17630–17635 (2009).
12. W. Liu, L. Pang, H. Han, W. Tian, H. Chen, M. Lei, P. Yan, and Z. Wei, "70-fs mode-locked erbium-doped fiber laser with topological insulator," Sci. Rep. **5**, 19997 (2016).
13. F. N. Xia, H. Wang, D. Xiao, M. Dubey, and A. Ramasubramaniam, "Two-dimensional material nanophotonics," Nat. Photonics **8**(12), 899–907 (2014).

#283063 https://doi.org/10.1364/OE.25.002950
Journal © 2017 Received 19 Dec 2016; revised 21 Jan 2017; accepted 27 Jan 2017; published 3 Feb 2017

Optics EXPRESS

14. Z. P. Sun, A. Martinez, and F. Wang, "Optical modulators with 2D layered materials," Nat. Photonics **10**(4), 227–238 (2016).
15. H. R. Mu, Z. T. Wang, J. Yuan, S. Xiao, C. Y. Chen, Y. Chen, Y. Chen, J. C. Song, Y. S. Wang, Y. Z. Xue, H. Zhang, and Q. L. Bao, "Graphene-Bi_2Te_3 heterostructure as saturable absorber for short pulse generation," ACS Photonics **2**(7), 832–841 (2015).
16. J. Sotor, G. Sobon, W. Macherzynski, P. Paletko, and K. M. Abramski, "Black phosphorus saturable absorber for ultrashort pulse generation," Appl. Phys. Lett. **107**(5), 051108 (2015).
17. R. I. Woodward and E. J. R. Kelleher, "2D saturable absorbers for fibre lasers," Appl. Sci. **5**(4), 1440–1456 (2015).
18. G. Sobon, "Mode-locking of fiber lasers using novel two-dimensional nanomaterials: graphene and topological insulators," Photon. Res. **3**(2), A56–A63 (2015).
19. K. Park, J. Lee, Y. T. Lee, W. K. Choi, J. H. Lee, and Y. W. Song, "Black phosphorus saturable absorber for ultrafast mode-locked pulse laser via evanescent field interaction," Ann. Phys. (Berlin) **527**(11-12), 770–776 (2015).
20. K. S. Novoselov, A. K. Geim, S. V. Morozov, D. Jiang, Y. Zhang, S. V. Dubonos, I. V. Grigorieva, and A. A. Firsov, "Electric field effect in atomically thin carbon films," Science **306**(5696), 666–669 (2004).
21. K. S. Novoselov, V. I. Fal'ko, L. Colombo, P. R. Gellert, M. G. Schwab, and K. Kim, "A roadmap for graphene," Nature **490**(7419), 192–200 (2012).
22. A. K. Geim and K. S. Novoselov, "The rise of graphene," Nat. Mater. **6**(3), 183–191 (2007).
23. P. G. Yan, H. Chen, K. Y. Li, C. Y. Guo, S. C. Ruan, J. Z. Wang, J. F. Ding, X. J. Zhang, and T. Guo, "Q-switched fiber laser using a fiber-tip-integrated TI saturable absorption mirror," IEEE Photonics J. **8**, 1500506 (2016).
24. S. S. Huang, Y. G. Wang, P. G. Yan, G. L. Zhang, J. Q. Zhao, H. Q. Li, and R. Y. Lin, "High order harmonic mode-locking in an all-normal-dispersion Yb-doped fiber laser with a graphene oxide saturable absorber," Laser Phys. **24**(1), 015001 (2014).
25. P. Yan, R. Lin, S. Ruan, A. Liu, and H. Chen, "A 2.95 GHz, femtosecond passive harmonic mode-locked fiber laser based on evanescent field interaction with topological insulator film," Opt. Express **23**(1), 154–164 (2015).
26. F. Bonaccorso, Z. Sun, T. Hasan, and A. C. Ferrari, "Graphene photonics and optoelectronics," Nat. Photonics **4**(9), 611–622 (2010).
27. W. D. Tan, C. Y. Su, R. J. Knize, G. Q. Xie, L. J. Li, and D. Y. Tang, "Mode locking of ceramic Nd: yttrium aluminum garnet with graphene as a saturable absorber," Appl. Phys. Lett. **96**(3), 031106 (2010).
28. J. Liu, Y. G. Wang, Z. S. Qu, L. H. Zheng, L. B. Su, and J. Xu, "Graphene oxide absorber for 2 μm passive mode-locking Tm:$YAlO_3$ laser," Laser Phys. Lett. **9**(1), 15–19 (2012).
29. M. N. Cizmeciyan, J. W. Kim, S. Bae, B. H. Hong, F. Rotermund, and A. Sennaroglu, "Graphene mode-locked femtosecond Cr:ZnSe laser at 2500 nm," Opt. Lett. **38**(3), 341–343 (2013).
30. J. Sotor, I. Pasternak, A. Krajewska, W. Strupinski, and G. Sobon, "Sub-90 fs a stretched-pulse mode-locked fiber laser based on a graphene saturable absorber," Opt. Express **23**(21), 27503–27508 (2015).
31. J. Boguslawski, J. Sotor, G. Sobon, R. Kozinski, K. Librant, M. Aksienionek, L. Lipinska, and K. M. Abramski, "Graphene oxide paper as a saturable absorber for Er- and Tm-doped fiber lasers," Photon. Res. **3**(4), 119–124 (2015).
32. L. Gao, T. Zhu, Y. J. Li, W. Huang, and M. Liu, "Watt-level ultrafast fiber laser based on weak evanescent interaction with reduced graphene oxide," IEEE Photonics Technol. Lett. **28**(11), 1245–1248 (2016).
33. S. Lu, C. Zhao, Y. Zou, S. Chen, Y. Chen, Y. Li, H. Zhang, S. Wen, and D. Tang, "Third order nonlinear optical property of Bi_2Se_3," Opt. Express **21**(2), 2072–2082 (2013).
34. S. Q. Chen, C. J. Zhao, Y. Li, H. H. Huang, S. B. Lu, H. Zhang, and S. C. Wen, "Broadband optical and microwave nonlinear response in topological insulator," Opt. Mater. Express **4**(4), 587–596 (2014).
35. D. Hsieh, D. Qian, L. Wray, Y. Xia, Y. S. Hor, R. J. Cava, and M. Z. Hasan, "A topological Dirac insulator in a quantum spin Hall phase," Nature **452**(7190), 970–974 (2008).
36. H. Zhang, C. X. Liu, X. L. Qi, X. Dai, Z. Fang, and S. C. Zhang, "Topological insulators in Bi_2Se_3, Bi_2Te_3 and Sb_2Te_3 with a single Dirac cone on the surface," Nat. Phys. **5**(6), 438–442 (2009).
37. C. J. Zhao, H. Zhang, X. Qi, Y. Chen, Z. T. Wang, S. C. Wen, and D. Y. Tang, "Ultra-short pulse generation by a topological insulator based saturable absorber," Appl. Phys. Lett. **101**(21), 211106 (2012).
38. J. Lee, J. Koo, Y. M. Jhon, and J. H. Lee, "A femtosecond pulse erbium fiber laser incorporating a saturable absorber based on bulk-structured Bi_2Te_3 topological insulator," Opt. Express **22**(5), 6165–6173 (2014).
39. K. X. Li, Y. R. Song, Z. H. Yu, R. Q. Xu, Z. Y. Dou, and J. R. Tian, "L-band femtosecond fibre laser based on Bi_2Se_3 topological insulator," Laser Phys. Lett. **12**(10), 105103 (2015).
40. K. Wu, X. Zhang, J. Wang, and J. Chen, "463-MHz fundamental mode-locked fiber laser based on few-layer MoS_2 saturable absorber," Opt. Lett. **40**(7), 1374–1377 (2015).
41. D. Mao, X. She, B. Du, D. Yang, W. Zhang, K. Song, X. Cui, B. Jiang, T. Peng, and J. Zhao, "Erbium-doped fiber laser passively mode locked with few-layer WSe_2/$MoSe_2$ nanosheets," Sci. Rep. **6**, 23583 (2016).
42. M. Liu, X. W. Zheng, Y. L. Qi, H. Liu, A. P. Luo, Z. C. Luo, W. C. Xu, C. J. Zhao, and H. Zhang, "Microfiber-based few-layer MoS_2 saturable absorber for 2.5 GHz passively harmonic mode-locked fiber laser," Opt. Express **22**(19), 22841–22846 (2014).
43. B. Guo, Y. Yao, P. G. Yan, K. Xu, J. J. Liu, S. G. Wang, and Y. Li, "Dual-wavelength soliton mode-locked fiber laser with a WS_2-based fiber taper," IEEE Photonics Technol. Lett. **28**(3), 323–326 (2016).

44. A. P. Luo, M. Liu, X. D. Wang, Q. Y. Ning, W. C. Xu, and Z. C. Luo, "Few-layer MoS_2-deposited microfiber as highly nonlinear photonic device for pulse shaping in a fiber laser," Photon. Res. **3**(2), A69–A78 (2015).
45. P. G. Yan, A. J. Liu, Y. S. Chen, H. Chen, S. C. Ruan, C. Y. Guo, S. F. Chen, I. L. Li, H. P. Yang, J. G. Hu, and G. Z. Cao, "Microfiber-based WS_2-film saturable absorber for ultra-fast photonics," Opt. Mater. Express **5**(3), 479–489 (2015).
46. K. Wu, X. Zhang, J. Wang, X. Li, and J. Chen, "WS_2 as a saturable absorber for ultrafast photonic applications of mode-locked and Q-switched lasers," Opt. Express **23**(9), 11453–11461 (2015).
47. B. Chen, X. Zhang, K. Wu, H. Wang, J. Wang, and J. Chen, "Q-switched fiber laser based on transition metal dichalcogenides $MoS_{(2)}$, $MoSe_{(2)}$, $WS_{(2)}$, and $WSe_{(2)}$," Opt. Express **23**(20), 26723–26737 (2015).
48. K. F. Mak, C. Lee, J. Hone, J. Shan, and T. F. Heinz, "Atomically thin MoS_2: a new direct-gap semiconductor," Phys. Rev. Lett. **105**(13), 136805 (2010).
49. J. Zheng, H. Zhang, S. Dong, Y. Liu, C. T. Nai, H. S. Shin, H. Y. Jeong, B. Liu, and K. P. Loh, "High yield exfoliation of two-dimensional chalcogenides using sodium naphthalenide," Nat. Commun. **5**, 2995 (2014).
50. K. Wang, J. Wang, J. Fan, M. Lotya, A. O'Neill, D. Fox, Y. Feng, X. Zhang, B. Jiang, Q. Zhao, H. Zhang, J. N. Coleman, L. Zhang, and W. J. Blau, "Ultrafast saturable absorption of two-dimensional MoS_2 nanosheets," ACS Nano **7**(10), 9260–9267 (2013).
51. Z. Q. Luo, Y. Y. Li, M. Zhong, Y. Z. Huang, X. J. Wan, J. Peng, and J. Weng, "Nonlinear optical absorption of few-layer molybdenum diselenide ($MoSe_2$) for passively mode-locked soliton fiber laser," Photon. Res. **3**(3), A79–A86 (2015).
52. Z. Luo, D. Wu, B. Xu, H. Xu, Z. Cai, J. Peng, J. Weng, S. Xu, C. Zhu, F. Wang, Z. Sun, and H. Zhang, "Two-dimensional material-based saturable absorbers: towards compact visible-wavelength all-fiber pulsed lasers," Nanoscale **8**(2), 1066–1072 (2016).
53. Y. Huang, Z. Luo, Y. Li, M. Zhong, B. Xu, K. Che, H. Xu, Z. Cai, J. Peng, and J. Weng, "Widely-tunable, passively Q-switched erbium-doped fiber laser with few-layer MoS_2 saturable absorber," Opt. Express **22**(21), 25258–25266 (2014).
54. H. Liu, A. P. Luo, F. Z. Wang, R. Tang, M. Liu, Z. C. Luo, W. C. Xu, C. J. Zhao, and H. Zhang, "Femtosecond pulse erbium-doped fiber laser by a few-layer MoS_2 saturable absorber," Opt. Lett. **39**(15), 4591–4594 (2014).
55. D. Mao, Y. Wang, C. Ma, L. Han, B. Jiang, X. Gan, S. Hua, W. Zhang, T. Mei, and J. Zhao, "WS_2 mode-locked ultrafast fiber laser," Sci. Rep. **5**, 7965 (2015).
56. P. Yan, A. Liu, Y. Chen, J. Wang, S. Ruan, H. Chen, and J. Ding, "Passively mode-locked fiber laser by a cell-type WS_2 nanosheets saturable absorber," Sci. Rep. **5**, 12587 (2015).
57. G. Z. Wang, S. F. Zhang, X. Y. Zhang, L. Zhang, Y. Cheng, D. Fox, H. Z. Zhang, J. N. Coleman, W. J. Blau, and J. Wang, "Tunable nonlinear refractive index of two-dimensional MoS_2, WS_2, and $MoSe_2$ nanosheet dispersions," Photon. Res. **3**(2), A51–A55 (2015).
58. D. Mao, B. Du, D. Yang, S. Zhang, Y. Wang, W. Zhang, X. She, H. Cheng, H. Zeng, and J. Zhao, "Nonlinear saturable absorption of liquid-exfoliated molybdenum/tungsten ditelluride nanosheets," Small **12**(11), 1489–1497 (2016).
59. S. Zhang, N. Dong, N. McEvoy, M. O'Brien, S. Winters, N. C. Berner, C. Yim, Y. Li, X. Zhang, Z. Chen, L. Zhang, G. S. Duesberg, and J. Wang, "Direct observation of degenerate two-photon absorption and its saturation in WS_2 and MoS_2 monolayer and few-layer films," ACS Nano **9**(7), 7142–7150 (2015).
60. H. Chen, Y. Chen, J. Yin, X. Zhang, T. Guo, and P. Yan, "High-damage-resistant tungsten disulfide saturable absorber mirror for passively Q-switched fiber laser," Opt. Express **24**(15), 16287–16296 (2016).
61. X. Zhang, X. F. Qiao, W. Shi, J. B. Wu, D. S. Jiang, and P. H. Tan, "Phonon and Raman scattering of two-dimensional transition metal dichalcogenides from monolayer, multilayer to bulk material," Chem. Soc. Rev. **44**(9), 2757–2785 (2015).
62. G. L. Frey, R. Tenne, M. J. Matthews, M. S. Dresselhaus, and G. Dresselhaus, "Raman and resonance Raman investigation of MoS_2 nanoparticles," Phys. Rev. B **60**(4), 2883–2892 (1999).
63. H. R. Gutiérrez, N. Perea-López, A. L. Elías, A. Berkdemir, B. Wang, R. Lv, F. López-Urías, V. H. Crespi, H. Terrones, and M. Terrones, "Extraordinary room-temperature photoluminescence in triangular WS_2 monolayers," Nano Lett. **13**(8), 3447–3454 (2013).
64. D. Ma, Y. Cai, C. Zhou, W. Zong, L. Chen, and Z. Zhang, "37.4 fs pulse generation in an Er:fiber laser at a 225 MHz repetition rate," Opt. Lett. **35**(17), 2858–2860 (2010).

1. Introduction

Two dimensional (2D) material is a type of layered compounds, which are composed of the single layer or multiple layers of atoms [1]. They have attracted much attention in basic and applied researches to the construction of photonic devices [2, 3]. In the meanwhile, fiber lasers have been applied in such fields as optical communications, nonlinear optics and laser processing [4]. In all kinds of fiber lasers, passively mode-locked fiber lasers can be used to generate ultrashort pulses efficiently. There are two main techniques for passively mode-locked fiber lasers: nonlinear polarization evolution (NPE) technique and saturable absorbers (SAs) technique [5, 6].

Fiber lasers with the NPE technique have the advantages of ultrashort pulse duration and simple structure [4, 5]. However, compared to other mode locking mechanism, the relatively high pump power has been needed for the mode-locked operation. Besides, they have been influenced by environment conditions easily, and usually have the relatively high mode-locking threshold [7–19]. SAs, such as semiconductor saturable absorber mirrors (SESAMs) and 2D material SAs, can be used to overcome those disadvantages. SESAMs are relatively flexible for the design of the laser cavity, but the fabrication process of SESAMs is complicated, the price is expensive, the damage threshold is low, and the bandwidth is narrow [7, 8]. With the development of the material technology, 2D materials as broadband saturable absorption materials have been applied to the SAs preparation successfully, and 2D material SAs in fiber lasers have shown excellent performance [9–19].

Among 2D materials, graphene has earlier been applied to the preparation of SAs [20–25]. Based on graphene SAs, researchers have obtained mode-locked pulses at 1 μm, 1.5 μm, 2 μm, and 2.5 μm [26–32]. But the ability of the light modulation is weak. By increasing the number of graphene layers, we can get a higher modulation depth, but the non-saturable loss is enlarged, which may cause performance degradation of lasers [30–32]. Topological insulators (TIs), as another kind of 2D materials, have been proved to be saturated absorption properties [33–36]. With TIs SAs, mode-locked fiber lasers have also been demonstrated [37–39]. Followed by graphene and TIs, transition metal dichalcogenides (TMDs) have been widely studied as saturable absorption materials [40–53]. For the TMDs SAs, they possess bandgap tunability by reducing the layer number or introducing the defects [51]. Besides, the modulation depth increases with the decrease of the layer number. Under the condition of the same electron relaxation time, the output pulse duration becomes shorter with the increase of the modulation depth [54–56]. Results have indicated that the preparation of TMDs SAs with the strong nonlinearity and large modulation depth has been valuable to generate mode-locked pulses with the ultrashort pulse duration [54–60].

In this paper, tungsten disulfide (WS_2), as a type of TMDs, will be used as the saturable absorption material to prepare the SAs. Compared to other work on the WS_2 SA [45], we have improved the preparation method for the WS_2 SA, which has smaller waist diameter, longer fused zone, higher nonlinearity and larger modulation depth. In order to enhance the reliability of the WS_2 SA, the WS_2 material will be deposited on the tapered fiber. Besides, to avoid being oxidized of the WS_2, the WS_2 layer on the tapered fiber surface will be protected by the gold film. Based on the NPE and WS_2 SA technique, the mode-locked erbium-doped fiber (EDF) laser will be demonstrated, and optical properties of the WS_2 SA and fiber lasers will be measured. Although the hybrid mode-locked scheme has been reported in our previous work [12], the performance of WS_2 materials has never been verified in the hybrid mode-locked EDF lasers. Besides, the pulse duration is related to many factors, but the modulation depth plays a great role. Thus, it is necessary to enhance the modulation depth of SAs. The modulation depth of the WS_2 SA in this paper is larger than that of the Sb_2Te_3 SA in the previous work [12]. Moreover, in order to examine the influences of the WS_2 SA, the contrastive experiments with or without the WS_2 SA will be carried out.

2. Results and discussion

2.1 The WS_2 SA preparation and characterization

The WS_2 SA is composed of three parts: the tapered fiber, WS_2 nanomaterial, and gold film. The SMF-28e fiber is made into the tapered fiber by the fused biconical taper devices. The waist diameter of the tapered fiber is 12 μm, and the effective length of the fused zone is 3 mm. Using the pulsed laser deposition (PLD) method, the WS_2 is deposited on the fused zone of the tapered fiber. When the lights are propagated in the tapered fiber, they will leak out in the fused zone, and interact between the evanescent fields of the propagating lights. Through controlling the length of the fused zone, we can change the interaction length between the lights and WS_2. Besides, the different waist diameters of the tapered fibers can lead to different nonlinear effects. When the waist diameter is smaller, the nonlinearity of SAs will be stronger. In this paper, the waist diameter of the tapered fiber is 12 μm, which is quit frangible. In order to avoid being broken off and oxidized for WS_2 SAs, the WS_2 layer deposited on the tapered fiber is protected by the gold film. The microstructure and morphologies of the WS_2 SA are confirmed via scanning electron microscope (SEM) in Fig. 1. We can see that the fiber is the tapered fiber in Fig. 1(a), and there are some materials on the surface of the tapered fiber. Figure 1(b) is the enlarged part of the film surface of the tapered fiber. Wherein, it is found that the film surface of the WS_2 SA is uniformly covered with ~40 nm monodisperse WS_2 nanoparticles, indicating the superior dispersibility of the WS_2.

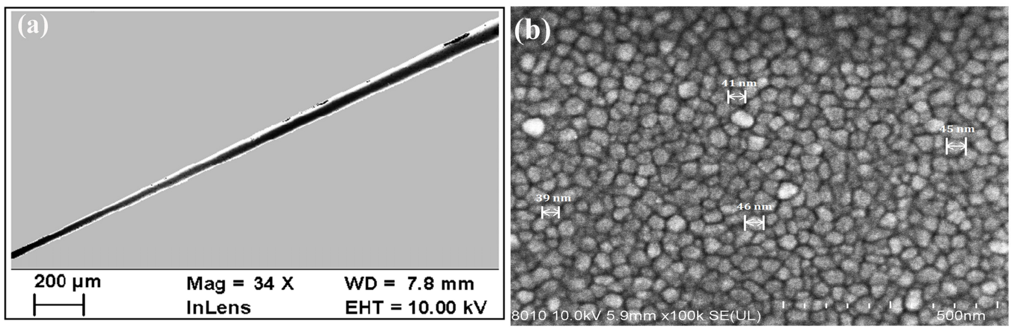

Fig. 1. (a) The SEM image for the taper waist of the WS_2 SA. The waist diameter is 12 μm, and the effective length of the fused zone is 3 mm. (b) Film surface of the WS_2 SA.

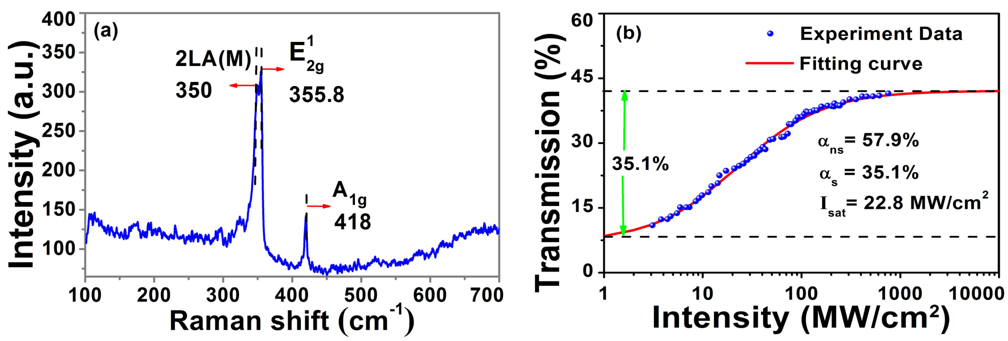

Fig. 2. (a) Raman spectrum of the WS_2 on the fiber-taper SA. Two optical phonon modes are at 355.8 cm^{-1} and 418 cm^{-1}, respectively. The typical longitudinal acoustic mode is at 350 cm^{-1}. (b) Nonlinear saturable absorption of the WS_2 SA. The modulation depth is 35.1%, the saturation intensity is 19.8 MW/cm^2, and the non-saturable loss is 59.5%.

In order to understand the atomic arrangement and measure the phonon spectrum of the WS_2 for the SA, we measure the Raman spectra as shown in Fig. 2(a). The lines observed at 355.8 cm^{-1} and 418 cm^{-1} correspond to E_{2g}^{1} and A_{1g} mode. The typical longitudinal acoustic mode is at 350 cm^{-1}. Those peaks correspond to the double-mode longitudinal acoustic feature due to the splitting in nanoparticles, in-plane inverse oscillation of W and S, and in-plane inverse oscillation between two S atoms of the WS_2 [61, 62]. All Raman characteristic peaks of the WS_2 correspond well to the previous researches [63], indicating the high purity of WS_2 nanoparticles on the fiber-taper SA. With the balanced twin-detector method in Fig. 3, we measure the nonlinear saturable absorption of the WS_2 SA. The pulse source is a homemade fiber laser with 1550 nm center wavelength, 80 MHz repetition rate and 200 fs pulse duration. Variable optical attenuator (VOA) is used to control the power level of an optical pulses through rotating the button above. As shown in Fig. 2(b), the modulation depth, saturation intensity and nonsaturable loss are measured to be 35.1%, 22.8 MW/cm^2 and 57.9%, respectively.

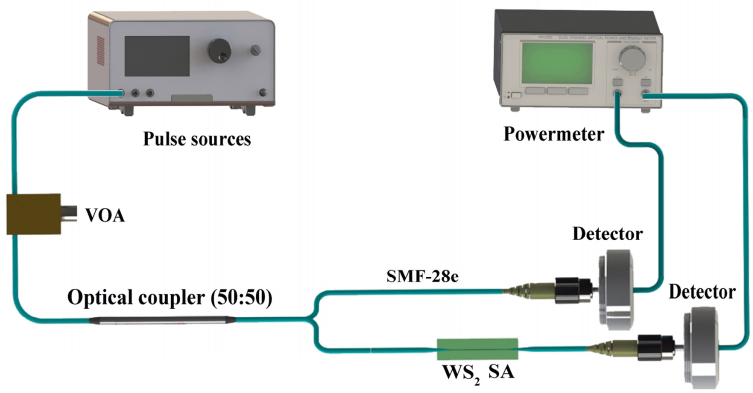

Fig. 3. Standard two-arm transmission setup.

2.2 Experimental setup

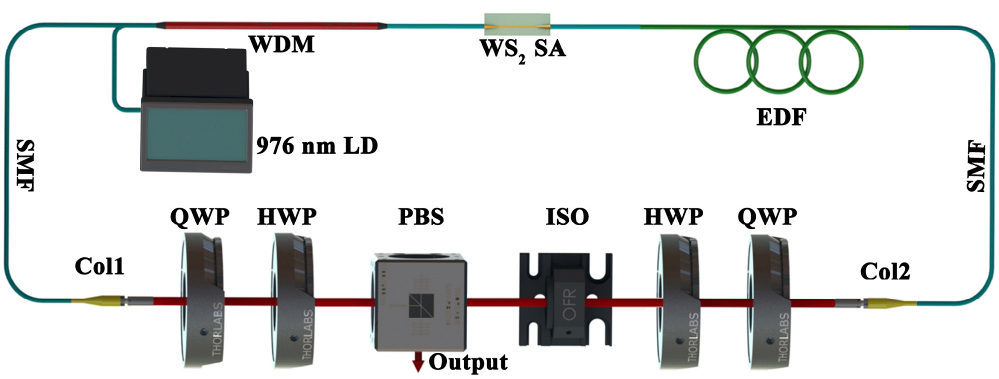

Fig. 4. Configuration of the passively mode-locked EDF laser with the fiber-taper WS_2 SA. LD is the laser diode, WDM is the wavelength-division multiplexer, SMF is the signal mode fiber, Col. is the collimator, QWP is the quarter wave plate, HWP is the half wave plate, PBS is the polarization beam splitter, ISO is the polarization-dependent isolator, and EDF is the erbium-doped fiber.

Figure 4 is the schematic diagram of the fiber laser. The ring cavity includes the 976 nm laser diode (LD, 680 mW maximum pump power), wavelength division multiplexer (WDM, 980 nm/1550 nm), fiber-taper WS_2 SA, erbium-doped fiber (EDF, Liekki 110-4/125, 12 fs^2/mm), single mode fiber (SMF, SMF-28e, –22 fs^2/mm), two fiber collimators, two half wave plates (HWP), two quarter wave plates (QWP), polarization-dependent isolator (ISO) and polarization beam splitting (PBS). In [12], Liu et al. have introduced how to use those optical devices. The total cavity length of the fiber laser is 1.54 m, and the repetition rate is about 135 MHz. The leading fibers of the WDM, collimators, and SA are all SMFs. The lengths of the EDF and SMFs are, respectively, 32 cm and 98 cm (25 cm for the WDM, 50 cm for the collimator, and 23 cm for the WS_2 SA). The free-space length of the ring cavity is about 22 cm. The net cavity dispersion is difficult to be determined because of the hybrid structure of the fiber-taper WS_2 SA, which is composed by the inner tapered fiber and the outer coated WS_2 film. Without the fiber-taper WS_2 SA, the fiber laser is a typical setup of fiber lasers with the NPE technique. In this paper, the fiber-taper WS_2 SA is added between the EDF and WDM. In this case, the mode-locked scheme of the fiber laser is a hybrid mode-locked scheme with the NPE and WS_2 SA technique. Compared to the typical NPE fiber laser, the

Optics EXPRESS

WS_2 SA in our fiber laser can be acted as the component to narrow pulse duration and reduce the mode-locked threshold.

2.3 Experimental results

Using the WS_2 SA, an all-fiber passively mode-locked EDF laser has been demonstrated without the NPE technique [45]. In this section, we mainly discuss the characteristics of EDF lasers with or without the WS_2 SA technique in Fig. 4, and highlight the importance of the WS_2 SA with the large modulation depth in the hybrid mode-locked EDF laser when the preparation method for the WS_2 SA is improved.

1) *EDF laser with NPE and WS_2 SA technique:* With NPE and WS_2 SA technique, the EDF laser can be mode-locked with the 87 mW pump power, which is the mode-locked threshold for our fiber laser. With 680 mW pump power and using an optical spectrum analyzer (Yokogawa AQ6315A), the central wavelength of the optical spectrum is measured to be 1540 nm, and the 3 dB spectral width is 114 nm in Fig. 5(a). With an optical intensity autocorrelator (Femtochrome, FR-103XL), the pulse duration is measured to be 67 fs as shown in Fig. 5(b).

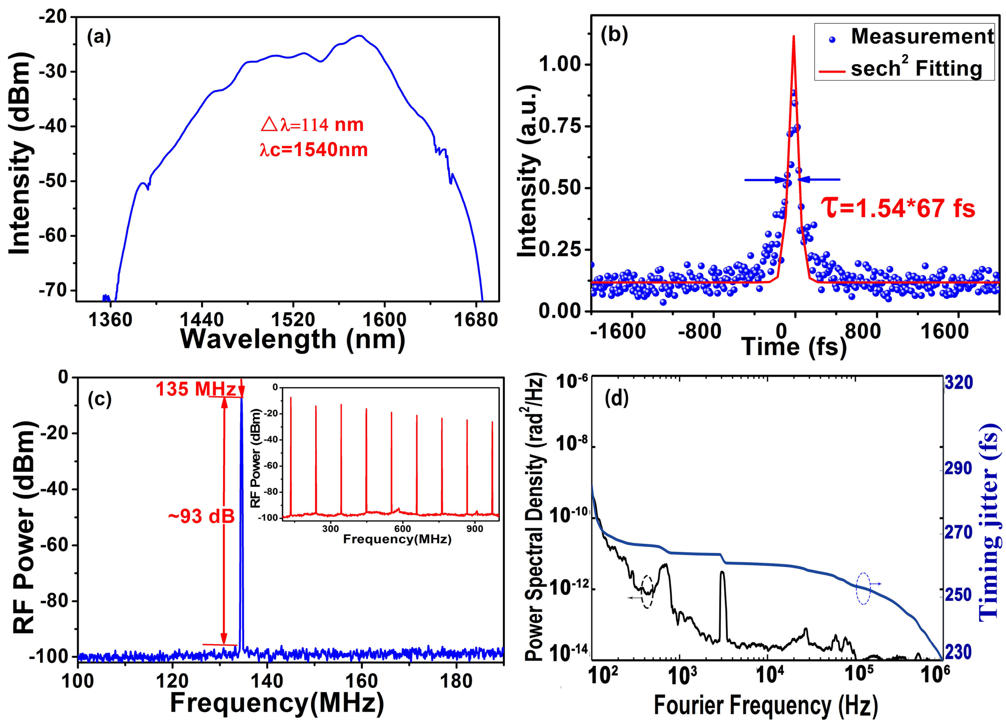

Fig. 5. Experimental results of the passively mode-locked EDF laser with the fiber-taper WS_2 SA. (a) Optical spectrum of the generated pulses. The 3 dB spectral width is 114 nm at 1540 nm. (b) Intensity autocorrelation trace with 67 fs pulse duration. (c) Radio frequency (RF) spectrum with 93 dB SNR measured with 10 kHz RBW. (d) Phase noise measurement at 135 MHz, and the timing jitter is about 290 fs.

Due to the high pump power, there is a small pedestal on the autocorrelation trace of Fig. 5(b). The repetition rate of the fiber laser is about 135 MHz in Fig. 5(c), which is measured by a radio frequency analyzer (ROHDE & SCHWARZ FSW26). With 10 kHz resolution bandwidth (RBW), the electrical signal to noise ratio (SNR) is measured to be 93 dB. Integrated from 1 MHz down to 100 Hz, we measure the timing jitter of the fiber laser is about 290 fs in Fig. 5(d), which indicates that the mode-locked state of the fiber laser is stable.

Optics EXPRESS

2) EDF laser with NPE technique: Only with the NPE technique, the EDF laser can also be mode locked. The problem "what role does the WS_2 SA play?" will be generated. In order to answer this question, we will use the SMF-28e fiber to replace the WS_2 SA under the same repetition rate. The corresponding results are presented in Fig. 6. The central wavelength of optical spectrum is a slight red shift to 1549 nm, and the 3 dB spectral width is reduced to 82 nm in Fig. 6(a). Correspondingly, the pulse duration increases to 95 fs, the SNR decreases to 85 dB, and the timing jitter increases to 950 fs. According to those results, we find that the WS_2 SA can be used to compress the pulse duration, increase the SNR, and decrease the timing jitter to enhance the stability of the fiber laser.

3) EDF laser with NPE and tapered fiber technique: In order to further emphasize WS_2's influence on the fiber-taper WS_2 SA, we replace the fiber-taper WS_2 SA with the same tapered fiber in Fig. 5, that is, the waist diameter is 12 μm, and the effective length of the fused zone is 3 mm. Figure 7 presents the corresponding measurement results. Compared to Fig. 6, the performances of the fiber laser continue to fall. The 3 dB spectral width is only 44 nm, the pulse duration becomes wider from 95 fs to 108 fs. Besides, the SNR continue to change as low as 80 dB. Due to the addition of the tapered fiber, the timing jitter increases to 15 ps. Those results indicate that the WS_2 has great influence on the WS_2 SA during the interaction between evanescent fields of propagating beams.

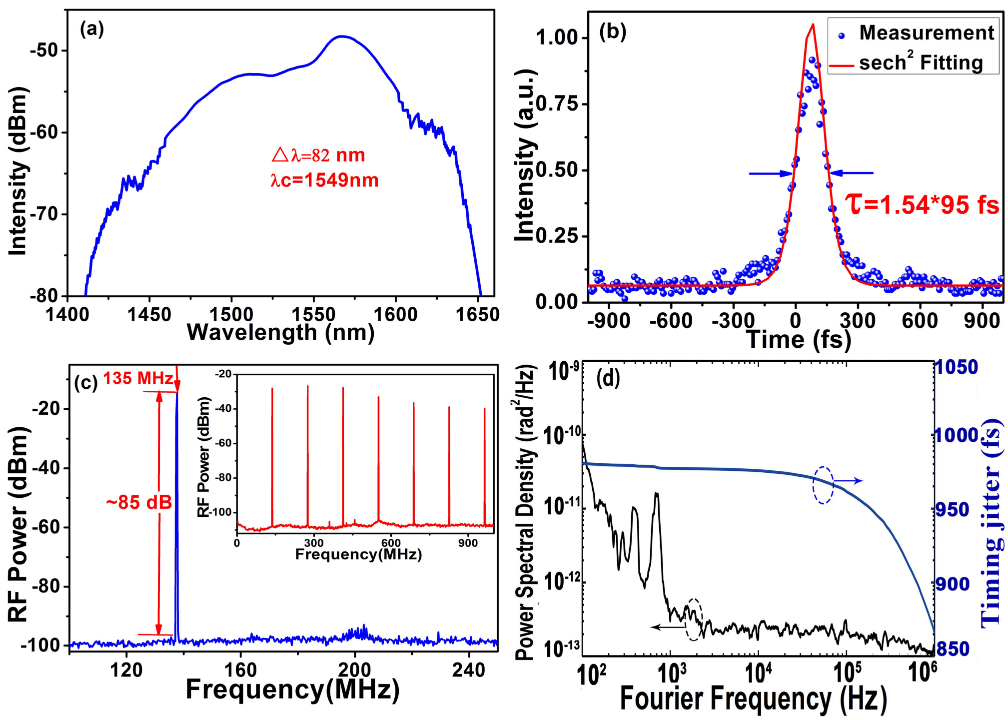

Fig. 6. Experimental results of the passively mode-locked EDF laser with the SMF in the same length. The difference with Fig. 4 is that the fiber-taper WS_2 SA is replaced with the SMF. (a) The 3 dB spectral width is 82 nm at 1549 nm. (b) Intensity autocorrelation trace with 95 fs pulse duration. (c) RF spectrum with 85 dB SNR measured with 10 kHz RBW. (d) Phase noise measurement at 135 MHz, and the timing jitter is about 0.95 ps.

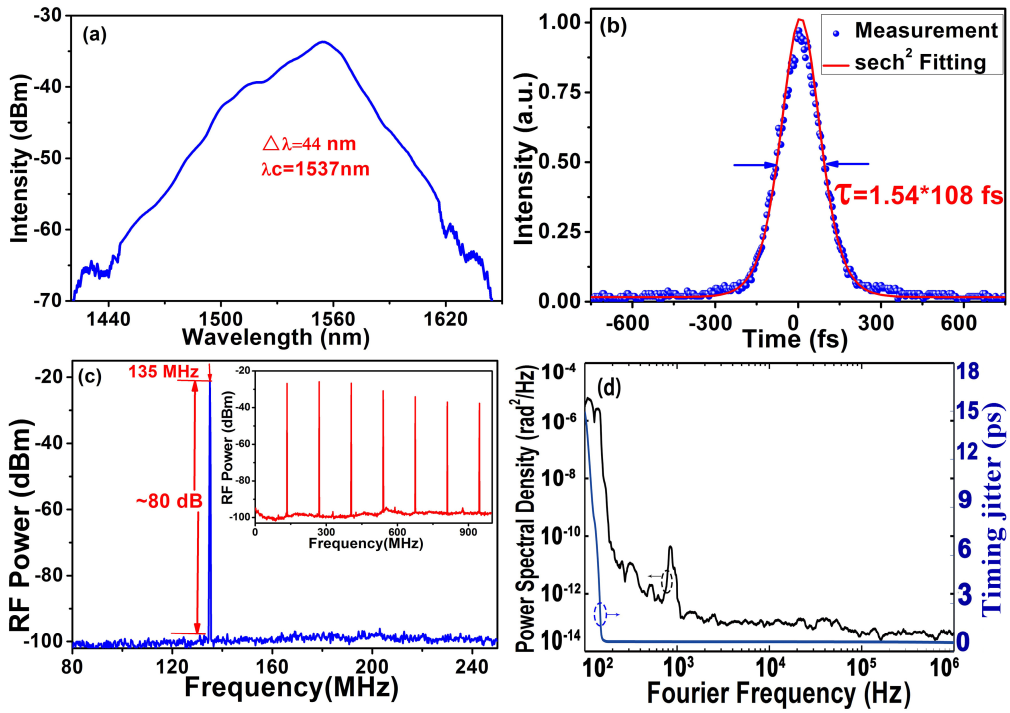

Fig. 7. Experimental results of the passively mode-locked EDF laser with the tapered fiber. The difference with Fig. 4 is that the fiber-taper WS_2 SA is replaced with the tapered fiber. (a) The 3 dB spectral width is 44 nm at 1537 nm. (b) Intensity autocorrelation trace with 108 fs pulse duration. (c) RF spectrum with 80 dB SNR measured with 10 kHz RBW. (d) Phase noise measurement at 135 MHz, and the timing jitter is about 15 ps.

According to above three experiments, we carry out the contrastive investigations on fiber lasers with or without the WS_2 SA, and the corresponding results are listed in Table 1. The enhancement of SNR indicates that the addition of the WS_2 SA can improve the stability of fiber laser. In addition, due to the large modulation depth, it is easier to get the shorter pulse than ever before. Furthermore, compared to other 2D material SAs in fiber lasers in Table 2, the 3 dB spectral width of this fiber laser is the widest, the SNR is the highest, the modulation depth is the largest, and the pulse duration is the shortest. Although 37.4 fs pulse generation from the EDF laser has been reported, the direct output pulse has been measured to be sub-100 fs [64], which is wider than 67 fs reported in this paper. Thus, the WS_2 SA with the large modulation depth is the excellent photonic device to shorten the pulse duration and optimize the related indicators of mode-locked fiber lasers.

Table 1. Summary of the parameters among mode-locked EDF lasers.

Mode-locking scheme	Spectral width (nm)	Pulse duration (fs)	SNR [dB]	Radio frequency (MHz)	Timing jitter (ps)
NPE + WS_2 SA	114	67	93	135	0.28
NPE	82	95	85	135	0.95
NPE + tapered fiber	44	108	80	135	15

Optics EXPRESS

Table 2. Comparison of mode-locked EDF lasers with SAs based on different materials. GO is the graphene oxide.

SA materials	Pulse duration (fs)	SNR (dB)	Spectral width (nm)	Modulation depth (%)	References
Carbon nanotubes	97.5	–	41.44	15.8	9
Graphene	88	65	48	4.8	30
Graphene oxide	613	69	4.2	1.4	31
Reduced GO	616	60	7.3	19	32
Sb_2Te_3	70	65	63	7.42	12
Bi_2Se_3	360	56	7.9	5.2	39
Black phosphorus	272	65	10.2	4.6	16
MoS_2	606	–	6.1	2.7	40
WSe_2	1250	–	2.1	0.5	41
WS_2	595	75	5.2	2.9	46
WS_2	67	93	114	35.1	This work

3. Conclusion

In this paper, the mode-locked EDF laser with the large modulation depth WS_2 SA has been demonstrated. With the PLD method, the fiber-taper WS_2 SA has been prepared. The modulation depth has been measured to be 35.1% with the balanced twin-detector method. The contrastive investigations on fiber lasers with or without the WS_2 SA have been conducted. With the WS_2 SA, the mode-locked pulse with 114 nm spectral width, 67 fs pulse duration, 93 dB SNR and 290 fs timing jitter has been obtained. To our knowledge, for mode-locked fiber lasers with 2D material SAs (such as graphene SAs, topological insulator SAs, and other 2D TMDs SAs), the 3 dB spectral width is the widest, the pulse duration is the shortest, the SNR is the highest, and the modulation depth is the largest in this paper. Results are helpful to exploit new photonic devices for fiber lasers with the wide spectrum, ultrashort pulse duration and high stability.

Funding

We thank the funding supports by the National Basic Research Program of China (973 Program Grant No. 2012CB821304), the National Natural Sciences Foundation of China (Grant Nos. 11674036, 11078022 and 61378040), and by the Fund of State Key Laboratory of Information Photonics and Optical Communications (Beijing University of Posts and Telecommunications, Grant No. IPOC2016ZT04).